Tellus (1982), *34*, 97–112

Stochastically-driven climatic fluctuations in the sea-ice, ocean temperature, CO_2 feedback system

By BARRY SALTZMAN, *Department of Geology and Geophysics, Yale University, New Haven CT 06511, U.S.A.*

(Manuscript received June 3; in final form August 19, 1981)

ABSTRACT

A simple climatic feedback system described previously (Saltzman and Moritz, 1980), involving sea-ice extent, mean ocean temperature and atmospheric CO_2, is modified in plausible ways to yield (1) a single stable equilibrium with slow periodic damping, and (2) auto-oscillatory (i.e., limit-cycle) behavior. These constitute two primary prototypical possibilities for the deterministic behavior of the real climatic system (others being the existence of *multiple* equilibria with assorted stabilities). The necessity for including stochastic forcing is discussed, and the role of this forcing in generating sustained irregular and quasi-periodic variability similar to that observed in the real system is illustrated. It is suggested that the spectral and "residence density" signatures of theoretical models such as these may be of value in identifying the deterministic phase space behaviour (e.g., number and nature of equilibria) underlying observed climatic variability, through an inspection of these signatures in real data.

1. Introduction

The variations of climate can be viewed as the output of a deterministic system with nonlinear feedbacks (expressed as a set of nonlinear ordinary differential equations governing the climatic variables averaged over some running time interval T) subject to the following inputs (cf., Fig. 1):

(i) external forcing of a relatively precise deterministic form (e.g., earth orbital radiation changes, or anthropogenic CO_2 changes),
(ii) external forcing of an imprecise, probabilistic form (e.g., atmospheric composition changes due to sequences of volcanic eruptions),
(iii) internal "forcing" of the average state due to the natural variability of the system variables on time scales smaller than T, and,
(iv) initial conditions representing the climatic state at some time which must also be imprecise to some degree.

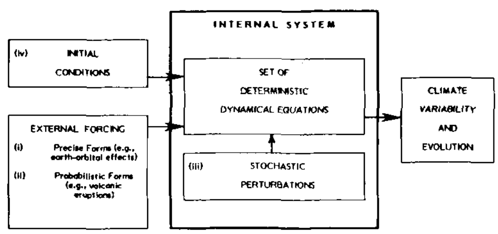

Fig. 1. Schematic flow chart showing the components of a theoretical model of climatic variability.

The internal forcing *(iii)* must be present if only due to the impossibility of fulfilling the Reynolds condition, $\overline{\partial\psi/\partial t} = \partial\bar{\psi}/\partial t$ (where the bar is the time average over T, ψ is an arbitrary climatic variable and t is time) cf., Robinson, 1978, but must also be present because of the impossibility of accounting completely for the effects of all the higher frequency variability through the physical parameterizations embodied in the deterministic model. If the deterministic model is well designed, containing enough of the relevant physics and relatively sound parameterizations, there is a good likelihood that the residual uncertainty expressed by this internal forcing (iii) can be represented as a "white noise" stochastic process. Given these

0040-2826/82/020097-16$02.50/0

probabilistic-stochastic components of the input, it is clear that the output climatic variations must also be of a probabilistic nature and can only be determined within some measure of uncertainty.

The output representing climatic change is conditioned strongly by the nature of the deterministic feedback processes, particularly the nature of the equilibrium states admitted. There are many possibilities, but we shall focus here on the following two prototypical scenarios discussed by Saltzman and Moritz (1980) (henceforth called S–M, 1980):

(1) The climatic system fluctuates near an *unstable* equilibrium associated with a dominant positive feedback near the equilibrium. Because of this instability the system can never settle down, but is prevented from running away catastrophically by powerful negative feedbacks that come into play and dominate when the departures from equilibrium become great. When more than one climatic variable is involved this tends to produce auto-oscillatory (i.e., limit-cycle) behavior.

(2) The climatic system fluctuates near a *stable* equilibrium associated with dominant negative feedback. The climate would reside permanently at this equilibrium were it not for variations in external forcing [(i) and (ii)] and internal stochastic forcing (iii) (cf., Hasselmann, 1976).

The first scenario was illustrated by Saltzman, Sutera and Evenson (1981) [henceforth called S–S–E (1981)] based on the simple system developed by the writer (S, 1978) and S–M (1980), involving the insulator properties of sea ice and a hypothetical relationship between atmospheric CO_2 and ocean temperature. In this S–S–E study an idealized model yielding a limit cycle solution was constructed on the basis of preliminary results that we will discuss in more detail in the present paper. The system was subjected to stochastic perturbations and the results, showing quasi-periodic, bimodal, almost-intransitive fluctuations, were presented in the form of sample time and phase plane evolutions as well as in the form of a "residence time" distribution expressing the probabilistic nature of the solution.

Another example illustrating this first scenario was given by Sutera (1981) who used a modified zero-dimensional Budkyo-Sellers model to show how an unstable equilibrium separating two stable equilibria could be "tunnelled" aperiodically to produce a bimodal climatic behavior. Similar behavior is also possible for special deterministic systems characterized by two unstable equilibria that act as "strange attractors" (Lorenz, 1963).

In the present study we return first to the original damped sea ice–ocean temperature oscillator model, S (1978), in which the destabilizing CO_2-temperature and ice-baroclinicity feedbacks introduced by S–M (1980) are absent, so that we have a system characterized by a dominant, stable equilibrium illustrative of scenario (2) above. Then we examine a modified form (i.e., Variant I) of the more detailed S–M (1980) model containing these positive feedbacks, but still having the property of admitting only one dominant stable equilibrium for plausible values of the physical parameters. We seek to demonstrate how a reasonable amount of stochastic forcing can make such systems containing a single stable equilibrium exhibit sustained, undamped, quasi-periodic variability that seems qualitatively similar to natural climatic records.

Finally, we present another modification of the S–M (1980) model (Variant II) that can yield a limit cycle solution, and again show the results of stochastic perturbations. As mentioned above, preliminary results from this model were the basis for the more idealized limit cycle model discussed by S–S–E (1981).

2. Three deterministic systems

2.1. *Model A [S, 1978]*

In seeking to illustrate the possibility for long term internal oscillations of the earth's climatic system of the type suggested qualitatively by Newell (1974) we are led, with extremely crude approximations, to a coupled system for the sine of the multi-annual mean sea ice latitude (η) and bulk ocean temperature (θ) of the form,

$$\frac{d\theta}{dt} = A\eta + B\eta^2 \equiv \Psi_A(\eta) \tag{1}$$

$$\frac{d\eta}{dt} = C + D\eta + E\theta \equiv \Phi_A(\eta, \theta) \tag{2}$$

The physical model leading to those equations is discussed in S (1978). For plausible estimates of the parameters involved we obtain the following values of the coefficients: $A = 414 \times 10^{-11}$ K s^{-1}, $B = -468 \times 10^{-11}$ K s^{-1}, $C = -111 \times 10^{-11}$ s^{-1}, $D = -627 \times 10^{-13}$ s^{-1} and $E = 420 \times 10^{-14}$ K^{-1} s^{-1}.

We found in S (1978) that these coefficient values yield a damped oscillation of period $P \approx 1550$ y and damping time constant $\tau \approx 1000$ y, approaching an equilibrium at $\eta_0 = 0.885$ (62.5° lat.) and $\theta_0 = 278$ K. A sample solution for the departures from this equilibrium, $\eta' = \eta - \eta_0$ and $\theta' = \theta - \theta_0$, in the form of a time evolution and a phase plane trajectory, is shown in Figs. 2A, B, respectively, starting from the arbitrary initial condition $\eta = 0.750$ ($\eta' = 0.135$) and $\theta' = 0$. A similar portrayal is also given and discussed in detail by Moritz (1979, case $\delta = 10^{-3}$). In part C of Fig. 2 we depict the "speed" of the trajectory, each dot being spaced at an equal time interval of 60 y.

2.2. *Model B [Variant I of S–M (1980)]*

An enlargement of the foregoing model was made in S–M (1980), including improvements in all the heat transfer parameterizations and an inclusion of CO_2 as a new variable. These changes enriched the feedback possibilities greatly, leading, in particular, to the presence of *positive* feedbacks (i.e., "ice-baroclinicity", and CO_2 and water vapor-temperature "greenhouse" effects) that were absent in the previous model.

This model, however, was unrealistic in at least two respects:

(1) Because the surface temperature was fixed at the equator, the north–south gradient could increase greatly as the ice advanced equatorward, leading to an enormous upward flux of sensible and latent heat from the ocean. The resulting oceanic cooling causes a further advance of the ice (i.e., the "ice-baroclinicity" positive feedback). We thus have the possibility for a runaway effect, manifested in the model by the existence of an unstable (saddle-point) equilibrium at $\eta_0 \approx 0.65$, $\theta_0 \approx 277.61$ K, along with a stable equilibrium similar to the one obtained in the previous model [$\eta_0 = 0.8783$ (61.5° lat.), $\theta_0 = 277.45$ K].

In reality we might expect that as ice approaches the equator the temperature at the equator should approach the fixed ice edge temperature 273 K. This would imply a reduction of the meridional temperature gradient for large equatorward displacements of the ice edge and hence a reduction or reversal of the instability due to this cause. To model such a possible temperature dependence we now replace the S–M (1980) formula for the surface temperature T_s as a function of the sine of the latitude ($\xi = \sin \varphi$) by the new formula

$$T_s(\xi) = \tau_s - a_s(1 + \xi^2 - \eta^2)^2 \tag{3}$$

where $\tau_s = 300$ K, $a_s = 28$ K. We continue to assume that the mean atmospheric lapse rate adjusts rapidly to a prescribed value so that the

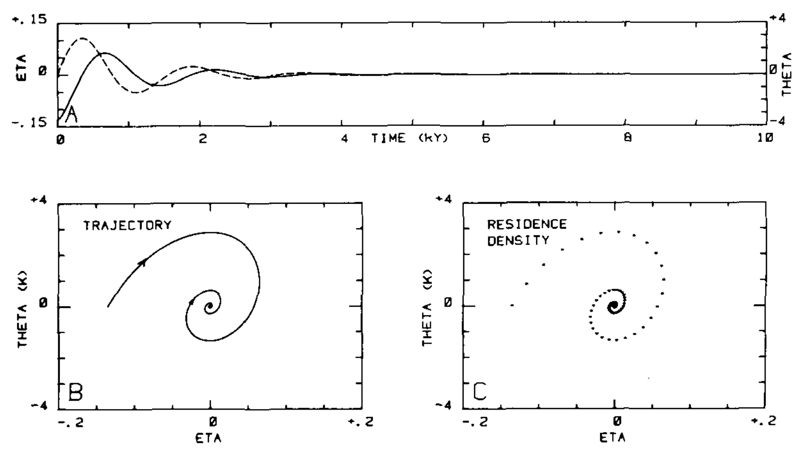

Fig. 2. Deterministic solution for Model A [S, 1978]. Top box (A): Sample time evolution of η' (full curve) and θ' (dashed curve). Lower left box (B): Phase plane trajectory of the sample solution shown in A. (Part C) Trajectory speed (dots are spaced at every 60 years).

meridional variation of the atmospheric temperature at level z above the surface, T_z, has a form similar to (3),

$$T_z(\xi) = \tau_z - a_z(1 + \xi^2 - \eta^2)^2 \quad (4)$$

where $\tau_z = 288.5$ K and $a_z = 28$ K. Note that (3) and (4) satisfy the condition that $(\partial T/\partial \varphi)_{\xi=0,1} = 0$.

(2) There is theoretical evidence that an increase in surface ice coverage is accompanied by a reduction of global cloud converage (cf., Paltridge, 1974; Gates, 1976), which is consistent with the observational fact that, at present, winter cloudiness is lower than summer cloudiness (cf., Schutz and Gates, 1971, 1972; van Loon, 1972). In the S–M (1980) model, however, we postulated a slight increase in cloudiness over all latitudes equatorward of advancing sea ice. To remedy this we adopt the following new formula for fractional cloud coverage n,

$$n(\xi) = N_0 + N_1\eta + N_2\eta^2 + N_3\frac{\xi^3}{\eta^3} \quad (5)$$

where $N_0 = 0.1$, $N_1 = 0.8$, $N_2 = -0.4$, and $N_3 = 0.4$.

With (3), (4) and (5) replacing formulas (2.1), (2.2) and (2.3) of S–M (1980), retaining all other formulations, we obtain after a lengthy though straightforward algebraic process the following system replacing (8.1) and (8.2) of that paper:

$$\frac{d\theta}{dt} = K_\theta\left(\sum_{j=0}^{14} \psi_j\eta^j + \theta\sum_{j=15}^{26} \psi_j\eta^{j-15}\right) \equiv \Psi_B(\eta, \theta) \quad (6)$$

$$\frac{d\eta}{dt} = K_\eta\left(\sum_{j=0}^{5} \phi_j\eta^j + \theta\sum_{j=6}^{8} \phi_j\eta^{j-6}\right) \equiv \Phi_B(\eta, \theta) \quad (7)$$

The values of the coefficients ψ_j, ϕ_j, obtained using all the same reference parameter values given by S–M (1980), are listed in Table 1. With these values, and again taking $K_\theta = 6 \times 10^{-11}$ K m^2 J^{-1} and $K_\eta = 6 \times 10^{-13}$ m^2 J^{-1}, we now find only a single physically meaningful equilibrium in the range $\theta \geq 273$, $0 \leq \eta \leq 1$, at $\eta_0 = 0.8498$ (58° lat.) and $\theta_0 = 278.68$ K. This equilibrium is stable. Due to our new surface temperature parameterization (3), the model no longer permits a strong ice baroclinicity feedback as the ice advances equatorward, as a consequence of which the unstable saddle point equilibrium of S–M (1980) is eliminated.

Table 1. *Reference values of the coefficients appearing in (6) and (7) (Variant I of S–M 1980)*

j	ψ_j	ϕ_j
0	−1.6380	−2723.000
1	110.0000	−7.545
2	−42.5000	−209.400
3	−210.6000	2.252
4	24.3500	39.480
5	−83.3700	79.650
6	−1.9940	10.210
7	87.7400	−0.162
8	12.3000	0.081
9	61.4000	
10	−1.5120	
11	−93.0900	
12	42.5900	
13	−8.7170	
14	0.6139	
15	−0.0051	
16	0.2702	
17	−0.1615	
18	0.2332	
19	−0.0878	
20	0.0247	
21	0.0109	
22	−0.0422	
23	0.0208	
24	−0.0022	
25	−0.0046	
26	0.0023	

The eigenvalues for this equilibrium, satisfying $(\theta', \eta') \sim e^{\omega t}$, are given by

$$\omega_\pm = a \pm \sqrt{a^2 - b} \quad (8)$$

where,

$$a = \frac{1}{2}\left(\frac{\partial\Psi}{\partial\theta} + \frac{\partial\Phi}{\partial\eta}\right)_{\eta_0,\theta_0}$$

$$= -8.79 \times 10^{-12}\ \mathrm{s}^{-1} \quad (9)$$

$$b = \left(\frac{\partial\Psi}{\partial\theta}\frac{\partial\Phi}{\partial\eta} - \frac{\partial\Psi}{\partial\eta}\frac{\partial\Phi}{\partial\theta}\right)_{\eta_0,\theta_0}$$

$$= 8.03 \times 10^{-20}\ \mathrm{s}^{-2} \quad (10)$$

Thus, we have a damped oscillation near this equilibrium, of period

$$P = \frac{2\pi}{(b - a^2)^{1/2}}$$

$$= 703\ \mathrm{y} \quad (11)$$

and damping time

$$\tau = -\frac{1}{a}$$

$$= 3612 \text{ y}. \qquad (12)$$

This damping time is longer than was obtained in the S (1978) model, indicative of a less stable equilibrium resulting from the presence of destabilizing positive feedbacks that were absent in the S (1978) model.

A sample time evolution and phase plane trajectory for the departures from this equilibrium (η', θ'), starting again from the initial conditions, $\eta = 0.75$ ($\eta' = 0.1$), $\theta' = 0$, is shown in Figs. 3A, B, respectively. As in Fig. 2, the speed of the trajectory is shown in Fig. 3C with each dot being spaced at an interval of 25 y.

Although this model appears to be more reasonable than S–M (1980) in the limit when $\eta \to 0$, a possible physical inconsistency is introduced that makes it, too, of questionable universal validity. In particular, the model allows the possibility that the ocean surface temperature decreases at the same time that the overall mean ocean temperature, θ, increases, a situation that is implausible (though not impossible). In spite of this possibility, the model is still of interest because it represents the prototype of a system having single stable equilibrium with a long damping time. We shall demonstrate how the stochastic perturbation of such a system can provide a sufficient source of instability to sustain quasi-periodic oscillations qualitatively similar to those revealed in climatic records.

2.2.1. *Bifurcation properties.* As was found in S–M (1980), this Variant I system undergoes a sequence of structural changes when we progressively reduce the value of the "inertia" parameter K_η from its reference value, 6×10^{-13} m^2 J^{-1} (that is, reduce the effectiveness of the ice-insulator negative feedback loop without changing the position of the equilibrium point). We find the following sequence of bifurcations: At first the system becomes less stable at the equilibrium point for small displacements and *un*stable for large displacements from equilibrium resulting in a small, hardly detectable, *un*stable limit cycle very close to the equilibrium point. A further reduction of K_η leads to an enlargement of the unstable limit cycle and the appearance of a new stable limit cycle very close to the equilibrium point which has become unstable. With a small further reduction of K_η, say to 2×10^{-13} m^2 J^{-1}, the small stable limit cycle disappears, leaving the system unstable for all displacements from the equilibrium point. This sequence has some of the properties of the so-called Landau-Hopf instability (e.g., McLaughlin and Martin, 1975).

A similar set of bifurcations is obtained if one fixes K_η and, instead, increases the parameter controlling the magnitude of the CO_2-longwave radiation positive feedback (i.e., the parameter b_{10} defined in S–M 1980).

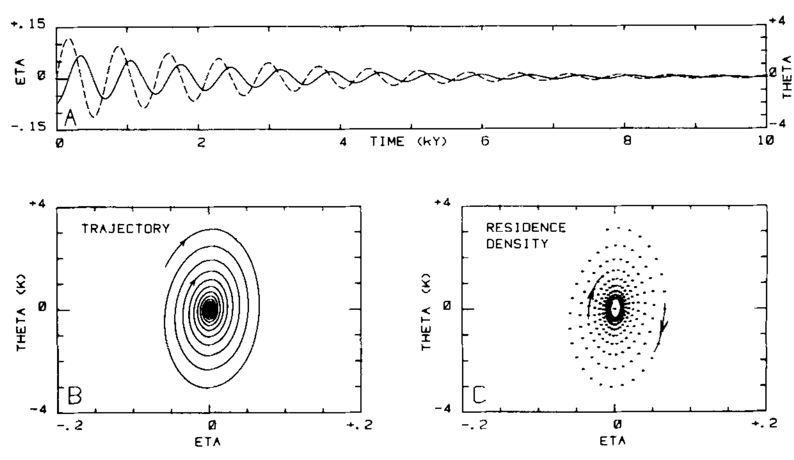

Fig. 3. Same as Fig. 2, for Model B [Variant I of S–M (1980)]. In Part C the dots are spaced at every 25 years.

In S–M (1980) we conjectured that a stable limit cycle should exist as a consequence of removing the strong ice-baroclinicity feedback that was inherent in the previous formula for T_s. However, in our present model B the appearance of the tiny stable limit cycle tightly enclosing the equilibrium hardly satisfies this expectation since the strong tendency for instability at large displacements and an *un*stable limit cycle are the most significant features of the model behavior. From a physical viewpoint, however, it seems more reasonable to expect that in the real climatic system there should be a stronger tendency for stability than instability for large displacements from equilibrium. As noted above, this seemingly unrealistic behavior arises because the new T_s-formulation (3) removes the positive ice-baroclinicity feedback for large near-equatorial displacements of ice only at the expense of simultaneously introducing a new source of positive feedback and instability, i.e., an intensification of the warming of the ocean when the ice advances due to the lowering of the surface water temperature as required by (3). This reinforces the effect of the ice-insulator process and magnifies the CO_2-positive feedback.

We are thus led to consider another formulation that is more physically plausible from this point of view, i.e., one in which the temperature of the surface water is compelled to increase as θ increases. In this case we must depend on the vertical heat transfer mechanisms in the model to provide the net cooling of the ocean necessary to supplement the ice-baroclinicity effect in dominating the CO_2-positive feedback at large θ. Such a new formulation, which we call Model C or Variant II of S–M (1980) is described next. As we shall see the formulation permits stable limit cycle behavior.

2.3. *Model C* [*Variant II of S–M* (*1980*)]

For the reasons given above we now propose to couple the equatorial surface temperature τ_s to the mean ocean temperature θ. Such a coupling seems physically plausible in view of the likelihood that the strong upwelling that tends to be induced dynamically near the equator reflects to some extent the bulk ocean temperature. We adopt the following modification of the S–M (1980) representations:

$$T_s(\xi) = \tau_s(\vartheta) - a_s(\vartheta)\frac{\xi^2}{\eta^2} \tag{13}$$

$$T_z(\xi) = \tau_z(\vartheta) - a_z(\vartheta)\frac{\xi^2}{\eta^2} \tag{14}$$

where

$$\vartheta = \theta - 277$$

$$\tau_s(\vartheta) = 300 + k_1\,\vartheta + k_2\,\vartheta^2 + k_3\,\vartheta^3$$

$$a_s(\vartheta) = \tau_s(\vartheta) - 273$$

$$\tau_z(\vartheta) = \tau_s(\vartheta) - 11.5$$

$$a_z(\vartheta) = a_s(\vartheta) = \tau_s(\vartheta) - 273$$

The quantities k_1, k_2, and k_3 are taken as constants, plausible values of which can only be speculated upon. Note that (13) and (14) again satisfy the constraint that $\partial T_{s,z}/\delta\varphi = 0$ at $\xi = 0, 1$. In this Variant II model we shall retain the original cloud representation used in S–M (1980), so that to recover the S–M (1980) model we have only to set $k_1 = k_2 = k_3 = 0$.

Although numerical experiments were performed with various values of k_1, k_2, and k_3, the most significant departure from the S–M (1980) results is obtained only when a cubic dependence of τ_s on ϑ is prescribed (i.e., $k_3 \neq 0$). In this case we have the possibility for limit cycle behavior illustrative of scenario (1) described in the Introduction. We shall here report the results corresponding only to the case $k_1 = 0$, $k_2 = 0$, $k_3 = 0.1$, in which the function $\tau_s(\vartheta)$ is as shown in Fig. 4.

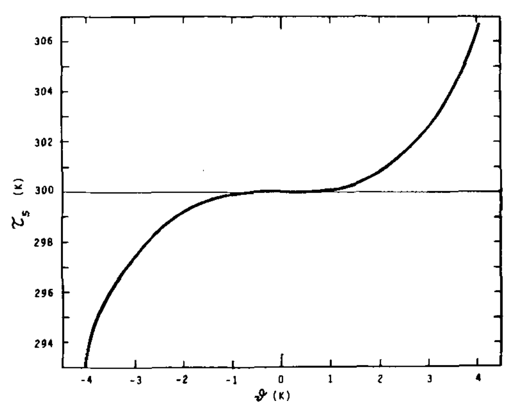

Fig. 4. Functional dependence of the equatorial surface temperature (τ_s) on ϑ, the departure of the mean ocean temperature from the reference value of 277 K, adopted in Model C [Variant II of S–M (1980)]: $\tau_s(\vartheta) = 300 + 0.1\vartheta^3$.

With this τ_s-representation, and with all other parameters fixed at the reference values given in S–M (1980) (e.g., $b_{10} = 0.001$, $A = 0.001$) we find that the system is nearly the same as in S–M (1980), having one stable equilibrium at ($\eta_0^{(1)} = 0.8904$, $\theta_0^{(1)} = 277.505$) and an unstable saddle-point equilibrium at ($\eta_0^{(2)} = 0.6469$, $\theta_0^{(2)} = 277.674$)—see Fig. 5. A sample time evolution and phase plane trajectory for departures (η', θ') from the stable equilibrium ($\eta_0^{(1)}$, $\theta_0^{(1)}$), starting from the initial condition $\eta = 0.75$ ($\eta' = 0.1$), $\theta' = 0$, is shown in Fig. 6.

However, when we increase b_{10} (the factor described in S–M (1980) controlling the magnitude of the positive feedback due to CO_2) to $b_{10} =$ 0.007 for example, a Hopf-bifurcation occurs, with the stable equilibrium point becoming unstable and shifting slightly to ($\eta_0^{(1)} = 0.9083$, $\theta_0^{(1)} = 277.598$). Because the system is still stable for somewhat larger displacements from this equilibrium (due to the increased warming and heat loss at the surface accompanying an increase in θ) we have the conditions for stable limit cycle behavior around this unstable equilibrium, as is illustrated in the complete phase plane picture shown in Fig. 7. Note that the unstable saddle-point equilibrium is still present here, in nearly the same position as in the reference case ($\eta_0^{(2)} = 0.6310$, $\theta_0^{(2)} = 277.849$). A sample time and phase plane evolution in the limit-cycle region is shown in Figs. 8A, D, respectively. In this figure we also show in parts B and C the variance spectra for η' and θ', respectively, plotted with the log of the variance per

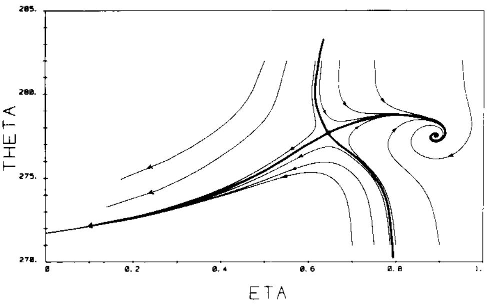

Fig. 5. Phase plane portrait for Model C [Variant II of S–M (1980); *Reference case* $b_{10} = 0.001$] showing the evolution of the state variables (η, θ) from any initial conditions. The two fixed points (i.e., equilibria) are shown by the dots.

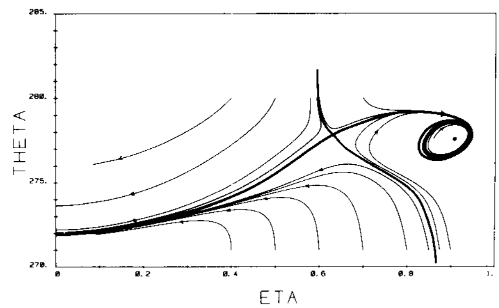

Fig. 7. Same as Fig. 5, for Model C *limit cycle case* ($b_{10} = 0.007$).

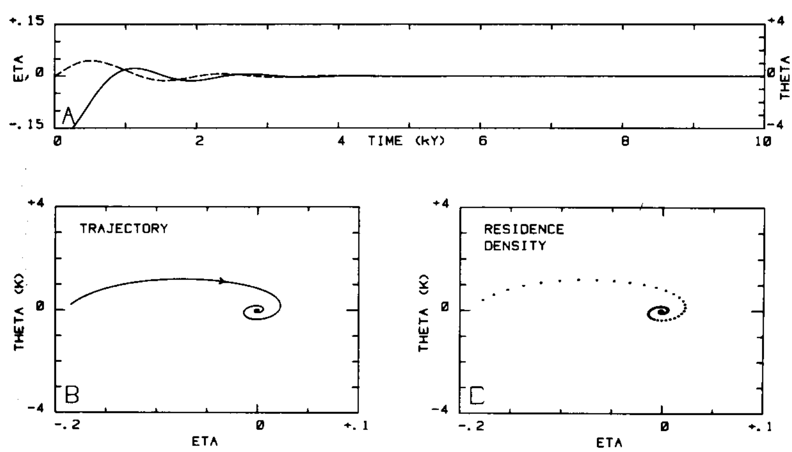

Fig. 6. Same as Fig. 2, for Model C [Variant II of S–M (1980); Reference case, $b_{10} = 0.001$]. η' and θ' are the departures from the stable equilibrium ($\eta_0^{(1)}$, $\theta_0^{(1)}$).

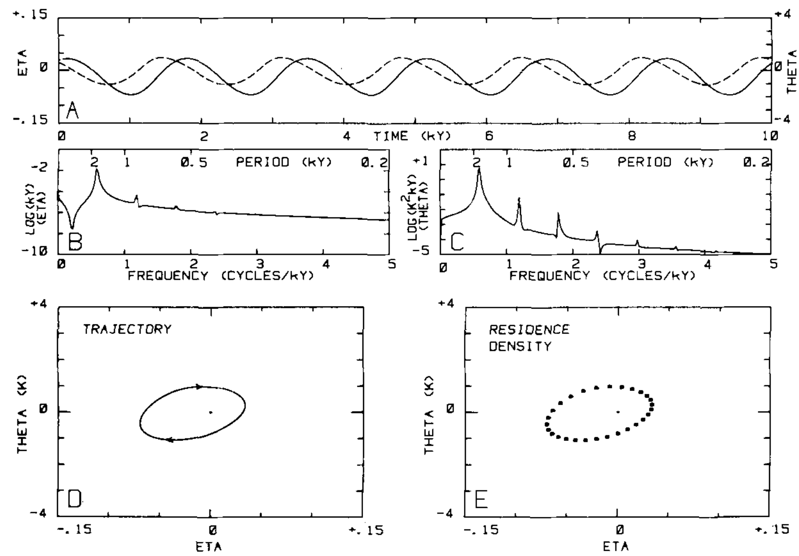

Fig. 8. Deterministic solution for Model C, limit cycle case, near the unstable equilibrium ($\eta_0^{(1)}$, $\theta_0^{(1)}$), showing the variance spectra for η and θ (parts B and C) in addition to the sample evolutions (part A), phase plane trajectory (part D), and trajectory speed shown by dots spaced at every 60 y (part E).

unit frequency (cycles/ky) as ordinates and both frequency (bottom) and period (top) as abscissa. In part E of the figure we portray the "residence density" of the solution, each dot again being spaced at an equal time interval of 60 y.

We can see that the system auto-oscillates with a period of about 1800 y, and amplitudes of about 1.0 K for θ' and about 0.050 for η' (i.e., roughly 6 deg lat). The relationship for the amplitude of the atmospheric carbon dioxide concentration corresponding to the θ'-variations is given by S–M (1980), and is of the form,

$$[CO_2]' = \frac{b_{10}}{b_8} [CO_2]^* \theta'$$

where $b_8 = 0.0235$, and $[CO_2]^*$ is a standard concentration (corresponding roughly to the equilibrium temperature) which we take to be 300 p.p.m. For $b_{10} = 0.007$ and $\theta' = 1.0$ K we find $[CO_2]' =$ 89.4 p.p.m., which is within the range of some recent estimates of CO_2 fluctuations accompanying ice ages (Delmas et al., 1980; Berner et al., 1980). An interesting feature is the asymmetry of the limit cycle with respect to the equilibrium point, the ice edge tending to move further to the equator than the pole from this point. Stated otherwise, there is greater stability for poleward excursions of the ice than for equatorward excursions. Also of interest is the tendency of the system to reside longer at the extreme positions of ice extent. As we have noted, on the basis of these results we constructed for preliminary analysis a simpler, prototypical, auto-oscillatory system representing the same physical processes included in this model (S–S–E, 1981).

3. Stochastic effects

3.1. *General considerations*

The deterministic systems described above are, at best, highly simplified and idealized models of the true climatic system, containing features that can only be regarded as speculative. Even if we assume, however, that these systems of equations correctly represent all of the significant physical processes operating on the time scales deduced (i.e., 10^3 y) they would still be incomplete because they fail to account fully for the natural variability known to exist on shorter time scales.

To demonstrate this, let us start with what we deem to be a rigorous physically-based equation for the variations of the ice edge extent η at any "instant". This, in fact, is a most difficult equation to formulate, but let us suppose it exists in a generalized form,

$$\frac{d\eta}{dt} = F(\eta, x_i; t) \tag{15}$$

where F represents all the relevant terms, linear and nonlinear, autonomous and non-autonomous, involving η and any other variables, $x_1, x_2, \ldots x_i \ldots$ that are necessary to account for the variations of η.

If we wish to use (15) to form an equation for the rate of change of a long-term running average value of η (i.e., a "climatic" mean value) in terms only of such climatic mean values we must proceed by averaging both sides of (15) over the averaging period T, which we define by a bar as follows

$$\bar{x}(t) = \frac{1}{T}\int_{t-T/2}^{t+T/2} x(\tau)\, d\tau \tag{16}$$

Thus, formally applying (16) to (15) we obtain

$$\overline{\frac{d\eta}{dt}} = \overline{F(\eta, x_i; t)} \tag{17}$$

For any interval $t = 0$ to T centered on $t = T/2$ we have

$$\overline{\frac{d\eta}{dt}} = \frac{1}{T}\int_0^T \frac{d\eta}{dt}\, dt = \frac{\eta(T) - \eta(0)}{T} \tag{18}$$

and, over this same interval we have

$$\frac{d\bar{\eta}}{dt} \approx \frac{\bar{\eta}(T) - \bar{\eta}(0)}{T} \tag{19}$$

Thus,

$$\overline{\frac{d\eta}{dt}} = \frac{d\bar{\eta}}{dt} - R_1 \tag{20}$$

where, assuming the origin is taken so that $\eta(0) = \bar{\eta}(0)$,

$$R_1 \approx \frac{1}{T}\left[\bar{\eta}(T) - \eta(T)\right] \tag{21}$$

As illustrated in Fig. 9, this correction factor R_1 will tend to be "random" if the high frequency departures $(\eta - \bar{\eta})$ from the running mean value are nonperiodic, and the magnitude of R_1 will typically range from zero to the amplitude (or standard deviation) of this departure divided by the averaging period T.

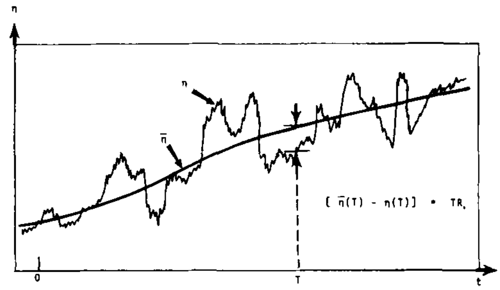

Fig. 9. Schematic representation of a possible variation of a climatic variable (say, η) and the running mean of that variable over a time interval T, $\bar{\eta}$, showing the random nature of the departure of the two quantities at $t = T$ assuming they are equal to $t = 0$.

In order to express the right hand side of (17) in terms of $\bar{\eta}$ and $\bar{x}_i$ we must use theory and/or observations to formulate (i.e., "parameterize") the nonlinear components of $\bar{F}$ in terms of these climatic means. In general, these parameterizations can be established satisfactorily only by considering an average over many higher frequency oscillations, this being a determining factor for the choice of T. Even for a sufficiently long period T, it is unlikely that anything more than approximate relationships subject to some error can be established. Moreover, it is also unlikely that all of the physical effects included in F will be treated in any given model, either by choice or through ignorance. Thus we have, in general,

$$\overline{F(\eta, x_i; t)} = \Phi(\bar{\eta}, \bar{x}_i; t) + E \tag{22}$$

where Φ is the "deterministic" part representing the physical processes explicitly modelled by means of some set of parameterizations, and E is an error function that includes both systematic (non-random) components due to omitted or misrepresented physical processes ϕ, and random components R_2, i.e., $E = \phi + R_2$. We can assume that the more complete and accurate we make the physical model embodied in Φ, the smaller ϕ will be and hence the more nearly random will E become.

Using (20) and (22) we obtain from (17) the following relation,

$$\frac{d\bar{\eta}}{dt} = \Phi(\bar{\eta}, \bar{x}_i; t) + \phi + S \tag{23}$$

where Φ is the deterministic part of $d\bar{\eta}/dt$, ϕ are systematic errors and $S = R_1 + R_2$ is the "stochastic" part comprising random noise associated with aperiodic, higher frequency variations. Thus, in the deterministic models discussed in the previous section we can identify η with $\bar{\eta}$ and the right hand sides of (2) and (7) with Φ, it being tacitly assumed in that section that $\phi = 0$ and $S = R_1 + R_2 = 0$.

However, from our analysis we know that even if we had an "exact" representation of all the deterministic physics (i.e., $E = 0$) there would still remain a residual random component R_1 due to the impossibility of fulfilling the so-called "Reynolds condition", $\overline{d\eta/dt} = d\bar{\eta}/dt$. If we assume that the random departures R_2 due to inaccuracies of the modelling approximations inherent in Φ are no greater than R_1, we can use observational evidence for R_1 to infer a reasonable amplitude for the stochastic "forcing" S that must be added to all the previous equations.

For purposes of calculation including this stochastic forcing, the previous deterministic equations are best generalized by expressing them in the so-called Itô-form (e.g., Schuss, 1980),

$$\delta\theta = \Psi(\eta, \theta)\, \delta t + \varepsilon_\theta^{1/2}\, \delta W \tag{24}$$

$$\delta\eta = \Phi(\eta, \theta)\, \delta t + \varepsilon_\eta^{1/2}\, \delta W \tag{25}$$

where $\delta\theta$ and $\delta\eta$ are increments of θ and η over a finite time increment δt, Ψ and Φ are the deterministic expressions described in the previous section, and

$$\varepsilon^{1/2}\, \delta W \equiv S \delta t \tag{26}$$

In (26) ε is the variance of $S\delta t$ (i.e., $\varepsilon^{1/2}$ is the standard deviation or, roughly, the typical amplitude of $S\delta t$) and δW is the incremental white-noise Wiener function that can be identified with the output of a random number generator of variance equal to one.

For illustrative purposes, in the following we shall assume that the stochastic forcing of the mean ocean temperature is of negligible amplitude ($S_\theta \approx 0$), but the mean sea-ice extent (which is known from observations to have significant variability) is subject to some stochastic forcing. We next obtain an estimate of the amplitude of such forcing, $\varepsilon_\eta^{1/2}$, assuming that R_1 is at least of comparable magnitude to R_2.

3.2. *Estimate of the stochastic amplitude of η*

According to Lemke et al. (1980) the observed interannual range of the annual mean sea-ice extent is about one third of the average seasonal range. Since this seasonal range is about 8 deg latitude, corresponding to a change in η of about 0.07, we may assume that a typical departure of an annual mean value of η from the longer term (say 10 y) average governed by our deterministic equations is of the order of 0.01. Thus, from (21), $R_1 \approx 0.01/10$ y $= 0.001$ y^{-1}, and taking $\delta t = 1$ y we have as our best-guess stochastic amplitude the value $\varepsilon_\eta^{1/2} \approx 0.001$. In order to explore the sensitivity of the response to this value we shall compute solutions for some values of $\varepsilon_\eta^{1/2}$ that are larger than this "standard" value.

4. Results with stochastic forcing

We now describe the results of integrating the stochastic systems (24) and (25) for the three deterministic systems described in Section 2 (Models A, B and C). In all cases we take $\varepsilon_\theta^{1/2} = 0$, and $\varepsilon_\eta^{1/2} \gtrsim 0.001$. All of these stochastic runs are made for a mimimum of 100,000 time steps (i.e., years, since $\delta t = 1$ y). The cases studied are listed in Table 2, and the results are portrayed in Figs. 10 to 13, using the same format as in Fig. 8. For these stochastic cases part (E) of these figures, in the lower right, is the "residence density" showing the number of yearly time steps per 10^4 y that the solution resides in an elementary region formed by a 60×60 grid of the phase plane.

Table 2. *Cases treated with stochastic forcing*

Deterministic model	Stochastic amplitude $\varepsilon_\eta^{1/2}$ (10^{-4})	Figure
A. S (1978)	10	10a
	20	10b
B. Variant I, S–M (1980)	10	11a
	20	11b
C. Variant II, S–M (1980) Reference Case	10	12a
	30	12b
Limit-Cycle Case ($b_{10} = 0.007$)	10	13a
	20	13b

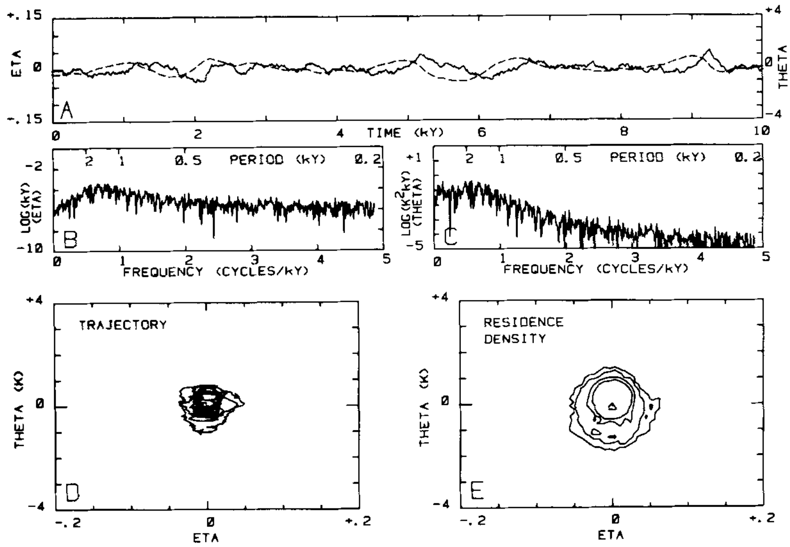

(a)

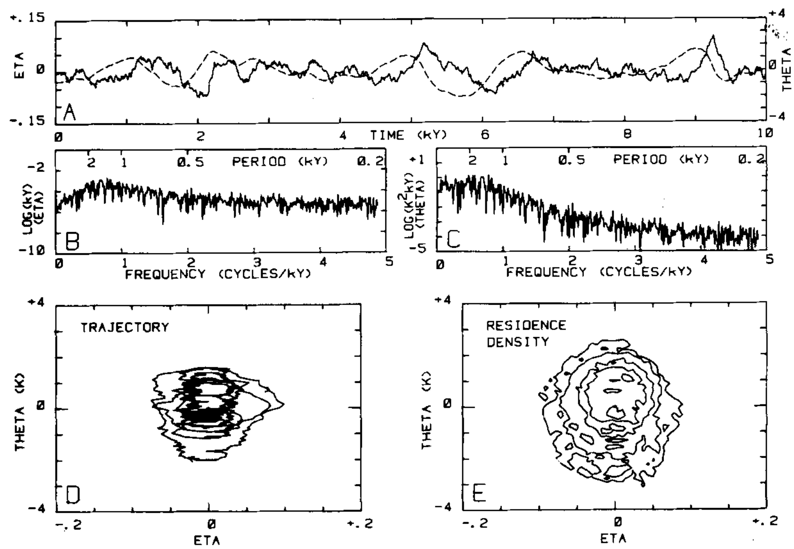

(b)

Fig. 10. Stochastic solutions for Model A [S (1978)], using the same format as in Fig. 8, for various stochastic amplitudes $\varepsilon_\eta^{1/2}$: (a) 10×10^{-4}, (b) 20×10^{-4}. The lower right box E now shows the "residence density" of the solution—i.e., the number of time steps (i.e., years) per 10^4 y that the trajectory resides in a region of the $\eta' - \theta'$ space. Proceeding inward toward the central maximum, the isolines in part E are in units of 0.5, 5, 25, 50, 200 for case (a); and 1.5, 5, 15, 25, 50 for case (b).

We can see from Figs. 10, 11, and 12 that the inclusion of a reasonable amount of stochastic forcing provides enough instability to prevent the system from relaxing to the deterministically *stable* equilibrium point, and can even lead to a sort of self-sustained, quasi-oscillatory behavior. Note the peaks in the spectra. This is illustrative of scenario (2) described in the Introduction.

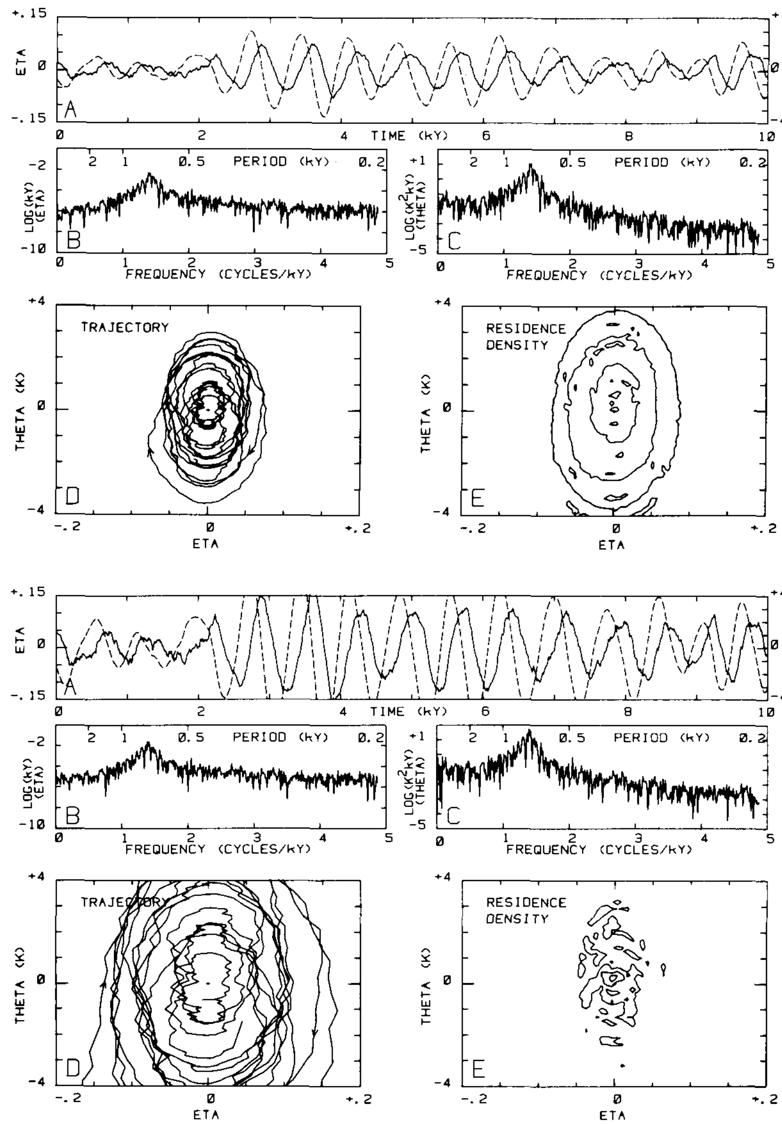

(a)

(b)

Fig. 11. Same as Fig. 10, for Model B [Variant I of S–M (1980)], for the following stochastic amplitudes $\varepsilon_\eta^{1/2}$: (a) 10 × 10^{-4}, (b) 20 × 10^{-4}. Proceeding inward toward the central maximum, the isolines in part E are in units of 1, 5, 20, 50 for case (a); and 7.5, 12.5, 20 for case (b).

In the S (1978) model (Fig. 10) and the Reference case of the Variant II (1980) model (Fig. 12), both of which are characterized by short damping times τ, a relatively high value of stochastic forcing (e.g., $\varepsilon_\eta^{1/2} \geqslant 0.002$) is needed to sustain a reasonable level of such quasi-oscillatory variability. However, for the Variant I (1980) model, characterized by a long damping time, the "standard" value of the stochastic amplitude ($\varepsilon_\eta^{1/2} = 0.001$) is adequate to maintain a quasi-periodic variation of the system. It would appear that a need exists for a good theoretical discussion of the criterion for such stochastically-forced quasi-periodic oscillations in stable dynamical systems. A

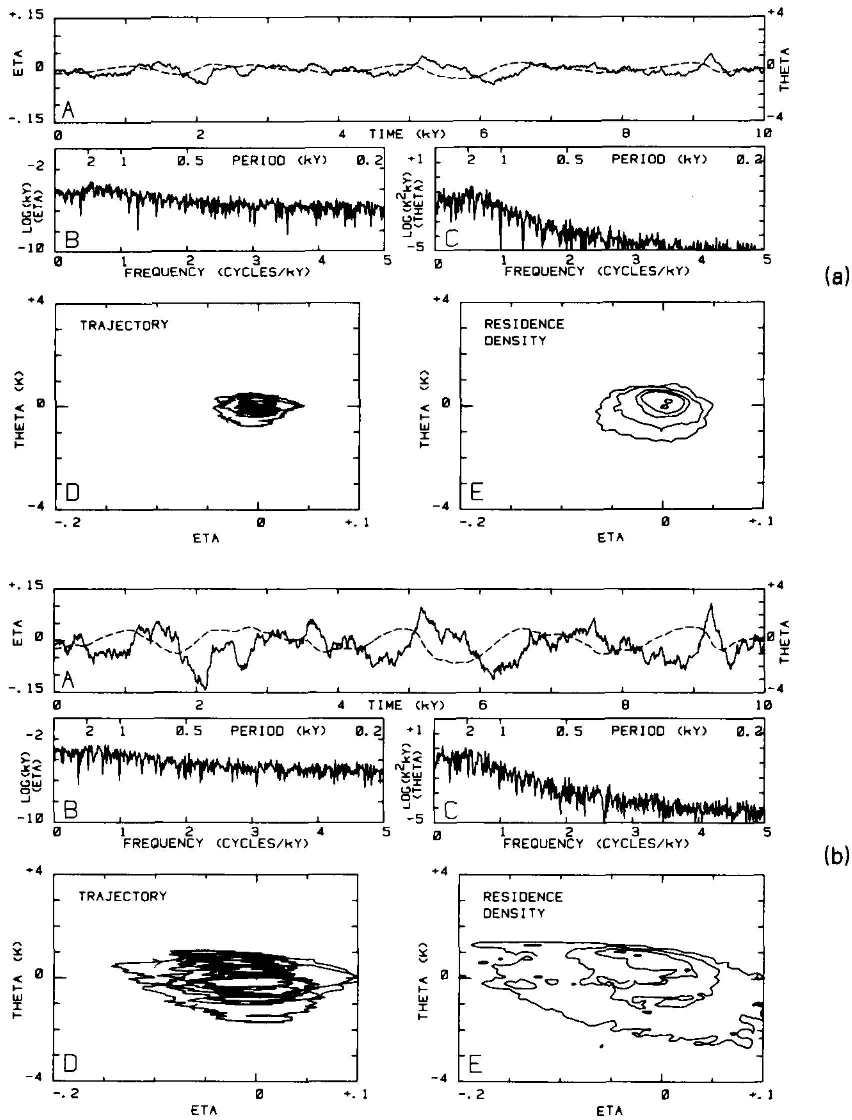

Fig. 12. Same as Fig. 10, for Model C [Variant II of S–M (1980); Reference case, $b_{10} = 0.001$], for the following stochastic amplitudes $\varepsilon_\eta^{1/2}$: (a) 10×10^{-4}, (b) 30×10^{-4}. Proceeding inward toward the central maximum, the isolines in part E are in units of 0.5, 10, 50, 100, 200 for case (a); and 1, 10, 30, 60 for case (b).

related discussion for auto-oscillating dynamical systems is given by Ebeling and Engel-Herbert (1980).

In spite of this tendency for quasi-periodic behavior, the attraction of the stable focus is still manifest, leaving a strong signature in the "residence density" portrait shown in part E of Figs. 10 and 11. Note the symmetry of this residence density about the equilibrium point. Although the system lies close to the equilibrium point much of the time, we find that a reasonable amount of stochastic noise can force irregular or quasi-periodic excursions of the ice edge of extent and time-scales known to have occurred on the earth

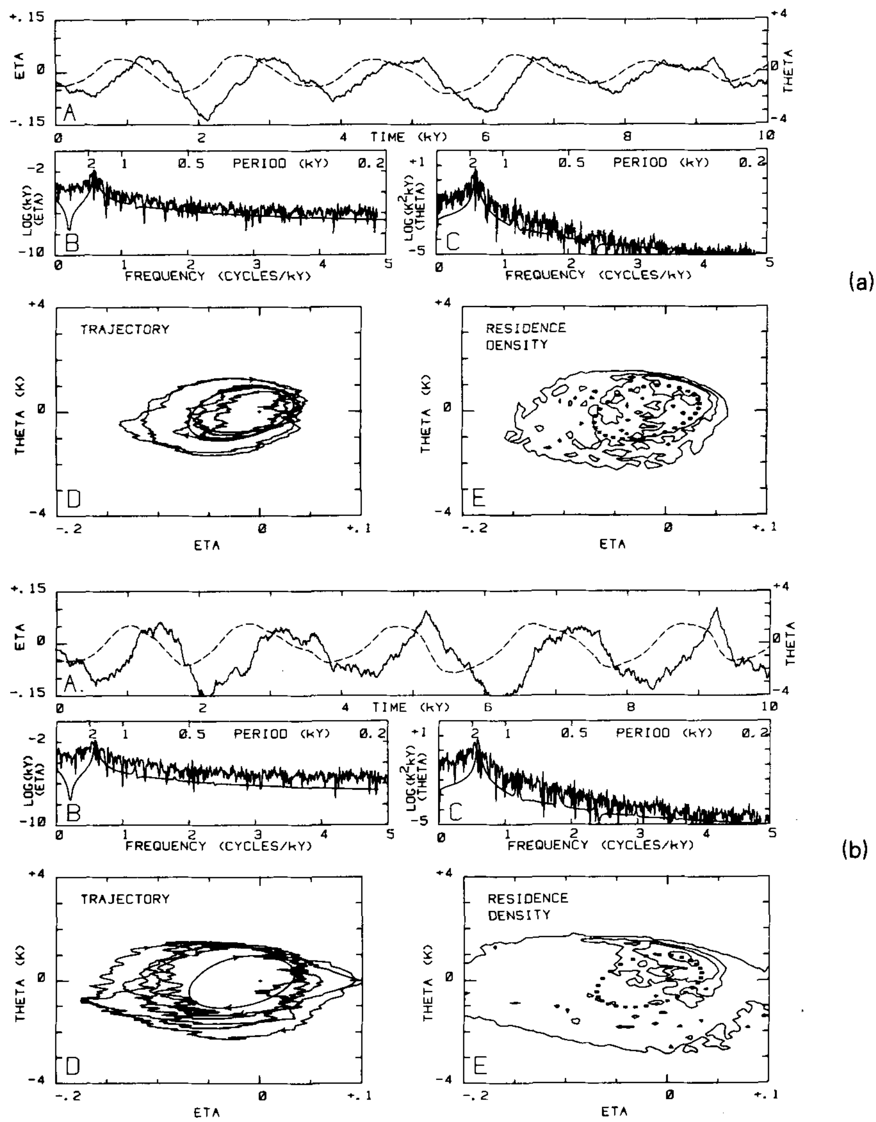

Fig. 13. Same as Fig. 10, for Model C [Variant II of S–M (1980); Limit cycle case, $b_{10} = 0.007$], for the following values of stochastic amplitudes $\varepsilon_\eta^{1/2}$: (a) 10×10^{-4}, (b) 20×10^{-4}. Proceeding inward toward the central maximum, the isolines in part E are in units of 1.5, 10, 20, 50 for case (a); and 0.5, 10, 20, 40 for case (b).

(i.e. the Little Ice Age variation)—see also Schnitker (1980). However, to corroborate our particular simple model as a plausible explanation of the observed ice edge fluctuation will require as a *necessary*, but not sufficient condition that some independent evidence be obtained showing that the mean ocean temperature (θ) varied simultaneously in proper phase with the ice edge.

An alternate scenario for climate variability [scenario (1) of the Introduction] is illustrated in Fig. 13, showing the effect of stochastic noise on a limit cycle deterministic trajectory. In this case the residence density is a maximum in the region of slow trajectory flow furthest from the equator. The poleward flow of the trajectories from the unstable saddle-point at $\eta_0^{(2)} = 0.63$, $\theta_0^{(2)} = 277.85$ K (see Fig. 7) tends to drive the stochastic solution to this region, leading to the interesting residence density signature shown in the Figure. In the idealized van der Pol-type model discussed in S–S–E (1981) this second saddle-point equilibrium was not present, with the result that the residence density was a maximum at both the equatorward and poleward regions of slow limit-cycle flow (i.e., a *bimodal*, almost intransitive, behavior was generated).

It is interesting to note the similarity in the residence density portraits shown in Figs. 12(b) and 13(b). This illustrates how both stable and unstable equilibria, separated by a bifurcation, can yield comparable signatures under the influence of stochastic noise. This was the point made by Sutera (1980) in his discussion of the Lorenz strange-attractor.

5. Conclusions

Using the simple climatic feedback system described in S (1978), and the extension of the more elaborate model described in S–M (1980), we have formed three deterministic systems that illustrate the following:

(a) A rapidly damped periodic approach to a stable equilibrium [Models A and C (Reference Case)]
(b) A slowly damped periodic approach to a stable equilibrium [Model B]
(c) Stable limit cycle flow around an unstable equilibrium [Model C ($b_{10} = 0.007$)].

It is clear that all three of the deterministic systems contain highly speculative elements and are not fully valid from a physical viewpoint, but Model C (Variant II of S–M 1980) is probably the most reasonable since only in this model is the ocean *surface* temperature required to bear some relationship to the overall mean ocean temperature. Notwithstanding all the possible physical inadequacies of these models, we can view the dynamical properties of these models as prototypes of those that are likely to arise in more complex and rigorous ones.

In particular, we have used three prototype systems to illustrate the effects of the stochastic noise that must be present in all models of climatic variability. We show, for example, how a reasonable amplitude of this stochastic noise can provide the instability to sustain the kind of irregular and quasi-periodic variability that seems characteristic of real climatic records, even when the deterministic system is stable. We also show how a limit-cycle type deterministic behavior is modified by the presence of stochastic noise to yield a more realistic variability.

As an outgrowth of these results we are led to entertain the possibility that by comparing the theoretical spectral and "residence density" signature for the various deterministic models (such as those treated here) with those generated by natural climatic records, some clues may be obtained concerning the underlying deterministic structure of the real system. As noted at the end of the last section, however, this is likely to be a most challenging task even for so fundamental a question as whether real climatic variability centers around a stable or unstable equilibrium, or near multiple equilibria. We note the appropriateness in this present context of the lines of Robert Frost quoted by Fleagle and Businger (1963) as the heading of their Chapter 1 on gravitational effects: "We dance round in a ring and suppose, But the Secret sits in the middle and knows".

6. Acknowledgements

This research was supported by the National Science Foundation under Grant ATM-7925013 (Climate Dynamics Program, Division of Atmospheric Sciences). I am grateful to Richard Moritz and Alfonso Sutera for useful discussions on this problem, to Alan Evenson for his original work in programming the computer graphics, and to Laurence Borten for his aid in making all of the calculations.

REFERENCES

Berner, W., Oeschger, W. H. and Stauffer, B. 1980. Information on the CO_2 cycle from ice core studies. *Radiocarbon 22*, 227–235.

Delmas, R. J., Ascencio, J.-M. and Legrand, M. 1980. Polar ice evidence that atmospheric CO_2 20,000 yr BP was 50% of present. *Nature 284*, 155–157.

Ebeling, W. and Engel-Herbert, H. 1980. The influence of external fluctuations on self-sustained temporal oscillations. *Physica 104A*, 378–396.

Fleagle, R. G. and Businger J. A. 1963. *An introduction to atmospheric physics*. Academic Press. 346 pp.

Gates, W. L. 1976. The numerical simulation of ice-age climate with a global general circulation model. *J. Atmos. Sci. 33*, 1844–1873.

Hasselmann, K. 1976. Stochastic climate models, part 1, theory. *Tellus 28*, 473–485.

Lemke, P., Trinkl, E. W. and Hasselmann, K. 1980. Stochastic dynamic analysis of polar sea ice variability. *J. Phys. Oceanogr. 10*, 2100–2120.

Lorenz, E. N. 1963. Deterministic non-periodic flow. *J. Atmos. Sci. 20*, 130–141.

McLaughlin, J. B. and Martin, P. C. 1975. Transition to turbulence in a statically stressed fluid system. *Phys. Rev. A12*, 186–203.

Moritz, R. E. 1979. Nonlinear analysis of a simple sea-ice ocean temperature oscillator model. *J. Geophys. Res. 84*, 4916–4920.

Newell, R. E. 1974. Changes in the poleward energy flux by the atmosphere and ocean as a possible cause for ice ages. *Quaternary Res. 4*, 117–127.

Paltridge, G. W. 1974. Global cloud cover and earth surface temperature. *J. Atmos. Sci. 31*, 156–160.

Robinson, G. D. 1978. Weather and climate forecasting as problems in hydrodynamics. *Mon. Weath. Rev. 106*, 448–457.

Saltzman, B. 1978. A survey of statistical-dynamical models of the terrestrial climate. *Advances in Geophysics 20*, 183–304.

Saltzman, B. and Moritz, R. E. 1980. A time-dependent climatic feedback system involving sea-ice extent, ocean temperature, and CO_2. *Tellus 32*, 93–118.

Saltzman, B., Sutera, A. and Evenson, A. 1981. Structural stochastic stability of a simple auto-oscillatory climatic feedback system. *J. Atmos. Sci. 38*, 494–503.

Schnitker, D. 1980. Fluctuations of oceanic deep water circulation—a cause of climatic cycles? (abstract). *EOS 61*, 983.

Schuss, Z. 1980. Singular perturbation methods in stochastic differential equations of mathematical physics. *SIAM Review 22*, 119–155.

Schutz, C. and Gates, W. L. 1971. *Global climatic data for surface, 800 mb, 400 mb: January*. The Rand Corp., Santa Monica, Calif., R-915-ARPA, pp. 173.

Schutz, C. and Gates, W. L. 1972. *Global climatic data for surface, 800 mb, 400 mb: July*. The Rand Corp., Santa Monica, Calif., R-1029-ARPA, pp. 180.

Sutera, A. 1980. Stochastic perturbation of a pure convective motion. *J. Atmos. Sci. 37*, 245–249.

Sutera, A. 1981. On stochastic perturbation and long-term climate behavior. *Quart. J. Roy. Met. Soc. 107*, 137–151.

van Loon, H. 1972. Cloudiness and precipitation in the Southern Hemisphere. *Meterological Monographs No. 35* (Meteorology of the Southern Hemisphere), *13*, 101–111.